Proceedings of the 2nd Marine Energy Technology Symposium
METS2014
April 15-18, 2014, Seattle, WA

MODEL PREDICTIVE AND INTEGRAL ERROR TRACKING CONTROL OF A VERTICAL AXIS PENDULUM WAVE ENERGY CONVERTER

Blake C. Boren*, Belinda A. Batten, and Robert K. Paasch

School of Mechanical, Industrial & Manufacturing Engineering
Northwest National Marine Renewable Energy Center
Oregon State University
Corvallis, Oregon
United States of America

ABSTRACT

By actively controlling the rotation of its pendulum, a vertical axis pendulum wave energy converter can generate significantly more net electricity from ocean waves than what would otherwise be possible through a passively swinging pendulum. This suggests that such converters can optimize their performance by incorporating active control schemes within their ever–changing ocean wave environment. The challenge of implementing such control, however, necessitates that an active controller be developed. Here, we address such challenges by: (i) deriving the equations of motion for a constrained generic vertical axis pendulum wave energy converter; (ii) modeling an irregular ocean wave environment; (iii) developing a model predictive and integral error tracking controller to enforce a desired control strategy; and (iv) simulating the converter within the modeled wave environment both with and without active control for the purpose of comparing their respective net power generation results. Here, we find that by actively controlling the rotation of the converter's pendulum, both continuous–mean and peak power generation are increased significantly. Simulation results show that active control is capable of increasing continuous–mean net power generation by over 200 percent. These results give strong evidence and support for further vertical axis pendulum wave energy converter development and also for the continued investigation of applying such active controllers to real world scenarios and prototypes.

*Corresponding Author: borenb@engr.orst.edu

NOMENCLATURE

(X_0, Y_0, Z_0)	global coordinate system, origin at still water level
(X_1, Y_1, Z_1)	hull fixed coordinate system
(X_2, Y_2, Z_2)	pendulum fixed coordinate system
$\vec{H}$	position vector of hull's center of mass
$\vec{P}$	position vector of pendulum's center of mass
$\vec{P}_H$	position vector of pendulum's center of mass w.r.t. hull
ω_{x1}	angular velocity of hull about X_1 axis
ω_{y1}	angular velocity of hull about Y_1 axis
ϕ	first Euler angle
θ	second Euler angle
ψ	third Euler angle
α	angular position of pendulum about Z_1 axis w.r.t. X_1 axis
m_h	mass of hull
I_{x1}	hull principal moment of inertia about X_1 axis
I_{y1}	hull principal moment of inertia about Y_1 axis
m_p	mass of pendulum
L	length of pendulum arm
g	acceleration due to gravity
$\vec{F}_E$	wave excitation force
$\vec{M}_E$	wave excitation moment
$\vec{F}_R$	hull radiation force
$\vec{M}_R$	hull radiation moment

$\vec{M}_d$ ..... pendulum moment due to viscous damping
$\vec{M}_{gen}$ ..... pendulum moment due to generator
$\vec{u}$ ..... pendulum control moment
R_{Py0} ..... coordinates of pendulum along global y axis
R_{Px0} ..... coordinates of pendulum along global x axis
C_{z0} ..... hull damping coefficient along Z_0 axis
C_{x1} ..... hull damping coefficient about X_1 axis
C_{y1} ..... hull damping coefficient about Y_1 axis
C_p ..... pendulum viscous damping coefficient about Z_1 axis
A_{z0} ..... added mass of hull along Z_0 axis
A_{x1} ..... added mass of hull about X_1 axis
A_{y1} ..... added mass of hull about Y_1 axis
H_{com} ..... hull center of mass
P_{com} ..... pendulum center of mass
η_j ..... water surface elevation of monochromatic wave j
k_j ..... wave number of monochromatic wave j
S ..... modified Bretschneider-Mitsuyasu wave spectrum
f_j ..... frequency [Hz] of monochromatic wave j
δ_j ..... phase of monochromatic wave j
K_{pj} ..... pressure response factor of monochromatic wave j
p_{irr} ..... pressure field of irregular wave
h ..... water depth
t ..... time
t_i ..... time window i
η_{irr} ..... water surface elevation of irregular wave
H_s ..... significant wave height
T_s ..... significant wave period
A, B, C, D ..... IDs of four hull wedges
$\vec{F}_N$ ..... excitation force of wedge ID N
A_f ..... sigmoid approximation factor
$\vec{d}_N$ ..... submergence of wedge ID N
$\vec{\eta}_N$ ..... water surface elevation at wedge ID N
$\vec{R}_N$ ..... position vector of wedge N w.r.t. hull
$\boldsymbol{\Upsilon}$ ..... state vector of model predicted pendulum system
$\boldsymbol{A}_{mpc}$. model predicted/approximated state matrix of pendulum
$\boldsymbol{B}$ ..... input matrix of model predicted pendulum system
$\boldsymbol{C}$ ..... output matrix of model predicted pendulum system
F_{Hz0} ..... overall vertical component of force acting on hull
$\dot{e}$ ..... error dynamics
$r(t)$ ..... tracking (reference) function
$\boldsymbol{\Upsilon}_{aug}$ ..... state vector of augmented system
$\boldsymbol{A}_{aug}$ ..... augmented system dynamics
$\boldsymbol{B}_{aug}$ ..... input matrix of augmented system
dotted variables, e.g. $\dot{\vec{v}}$ ..... time derivatives

INTRODUCTION

The world's oceans contain an abundance of energy in the form of waves. Converting such energy into electricity presents an attractive and sustainable opportunity to power communities and cities. To access, harvest, and then generate electricity from such an energy resource, however, currently requires techniques and technologies that are both nascent in nature and relatively expensive when compared to the status quo: coal and natural gas power plants [1]. There exists a need, therefore, to reduce the cost of generating electricity from ocean waves by further developing and finding more cost effective conversion devices and techniques [2]. Here, we address this need by focusing on the continued development of a specific type of wave energy converter known as a vertical axis pendulum wave energy converter, or VAPWEC, and applying active control to it.

A VAPWEC utilizes the motion of undulating ocean waves to induce tilting moments about its center of mass. These tilting moments cause the converter's pendulum to swing about an axis of rotation whose orientation would be vertical if the converter were placed on level ground. The swinging pendulum drives a generator to generate electricity. Collectively, the process of using tilting moments to swing a pendulum to drive a generator, is the basic archetype for any VAPWEC power take–off system.

The first VAPWEC was patented in 1966 by the Thiokol Chemical Corporation, see Figure 1 [3]. Originally intended for use as a self-powered marine navigation beacon, Thiokol's device is, nonetheless, a design that reflects the basic operation of any modern VAPWEC. Examples of modern, utility grid scale VEPWECs include those developed by companies such as Neptune Wave Power LLC and Wello Ltd.

VAPWECs have two noteworthy characteristics that contribute to their viability as wave energy converters and warrant their continued research and development: (i) in both very small and very large waves, VAPWECs can utilize the entire range of their power take–off system and (ii) all converter components (e.g., generator, gearbox, bearing, axle, and pendulum) are housed within a protective hull. In other words, the hull of the VAPWEC need only be slightly tilted to induce pendulum motion, and that motion is unrestricted regardless of sea state. Furthermore, by enclosing all components within the VAPWEC's hull, the components are protected from the harsh, corrosive ocean wave environment, thus extending device longevity and reducing device maintenance. Nevertheless, while the aforementioned VAPWEC characteristics are significant, there exists further opportunity to enhance the converter by actively controlling

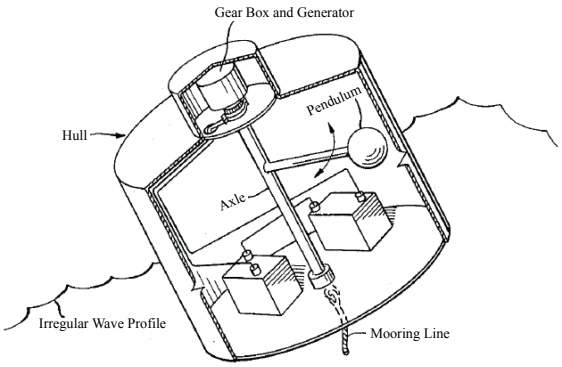

FIGURE 1. BASIC OPERATION OF A VAPWEC. FIRST PATENTED IN 1966 BY THE THIOKOL CHEMICAL CORPORATION [3]. PUBLIC DOMAIN: SEE U.S. PATENT NUMBER 3231749.

the motion of its pendulum [1, 2].

Any random motion of a VAPWEC's pendulum will drive its generator to produce electricity, but in an irregular ocean environment, it is unlikely to produce power at optimal levels. One way to improve the converter's performance is to identify an improved or more ideal pendulum motion trajectory. For example, one can first identify superior pendulum motion trajectories for a series of ocean sea states and then effectuate such motion when needed through application of active control. In this way, a VAPWEC can optimize its conversion performance thereby causing itself to become a more efficient and cost effective means of converting ocean wave energy into electricity. The challenge then, is: (i) to determine an optimal pendulum motion for a given irregular ocean wave environment and (ii) to then establish a means of effectuating such optimal pendulum motion through controlled actuation.

For regular monochromatic waves, Bretl identified an optimal pendulum state trajectory as having unidirectional rotation at the same angular frequency as the monochromatic wave [4]. For irregular waves, Boren proposed that optimal pendulum state trajectory be achieved by coinciding "maximum potential energy pendulum positions" with the crests and troughs of the spacial irregular wave form [5]. In this paper, we seek to build upon [4, 5] by specifically investigating the electric power generation gains of an actively controlled VAPWEC as compared to an uncontrolled VAPWEC. We accomplish this by (i) modeling a generic VAPWEC within a simulated ocean wave environment and (ii) by developing an active optimal controller based on model predictive and integral error tracking control theories capable of enforcing an optimal pendulum state trajectory.

In this approach, use of model predictive control provides a means to continually approximate the nonlinear pendulum dynamics for allotted time horizons in a way that enables the use of common linear optimal control methods. Moreover, model predictive control provides a means for future research in which temporal wave profile prediction can occur [6–8]. With integral error control aspects, the controller has the ability to track a desired ideal pendulum state trajectory and account for any errors due do approximating the pendulum's nonlinear dynamics. The controller combines the model predictive and integral error control aspects via an augmented state-space equation with an associated standard linear quadratic regulator (LQR) cost function.

METHODOLOGY

To develop and then investigate the effects of an active controller to enforce desired pendulum state trajectories we: (i) develop equations of motion that define a generic VAPWEC with four degrees of freedom (heave, roll, pitch, and pendulum rotation); (ii) develop a simulated irregular wave environment that WEC designers would use for converters deployed off the coast of Oregon (see [9]); (iii) develop a control strategy based on model predictive and integral error control for increased VAPWEC net power production; (iv) provide simulation results of an uncontrolled and controlled generic VAPWEC; and (v) offer conclusions and insights regarding future research prospects for continued VAPWEC development.

VAPWEC with Four Degrees of Freedom

The basic nature of essentially all WEC power take–off systems requires that relative motion occurs between at least two bodies. To ensure such relative motion, often one body is heavily constrained and damped. For VAPWECs, the primary mode of wave energy conversion is through the swing of a pendulum whose motion is caused by a tilting hull. Thus, while the VAPWEC's hull should both move up and down in heave, and tilt back and forth in roll/pitch, hull motion in surge is unnecessary and hull motion in yaw should be constrained.

Given an appropriate mooring scheme, the generic VAPWEC can be constrained to move in large part in only heave, roll, and pitch. Thus, with the inclusion of pendulum motion, the generic VAPWEC modeled has four dominant degrees of freedom. Figure 2 shows a free body diagram illustrating the dynamics of the constrained VAPWEC. The equations of motion for the VAPWEC are derived using Newtonian mechanics with the aid of three coordinate systems: global fixed, hull fixed, and pendulum fixed coordinate systems. Using the z-x'-z'' sequence, Euler angles ϕ, θ, and ψ are employed to relate the angular orientation of the VAPWEC's hull and, indirectly, the VAPWEC pendulum's position to the global coordinate system, see [10, 11]. Here we consider six main forces or moments affecting the VAPWEC: (i) wave excitation force $\vec{F}_E$ and moment $\vec{M}_E$; (ii) wave radiation force $\vec{F}_R$ and moment $\vec{M}_R$; (iii) weight of the hull $m_h\vec{g}$; (iv) weight of the pendulum $m_p\vec{g}$; (v) pendulum viscous damping moment $\vec{M}_d$; and (vi) pendulum generator moment $\vec{M}_{gen}$.

The equation of motion for the hull moving along the Z_0 axis

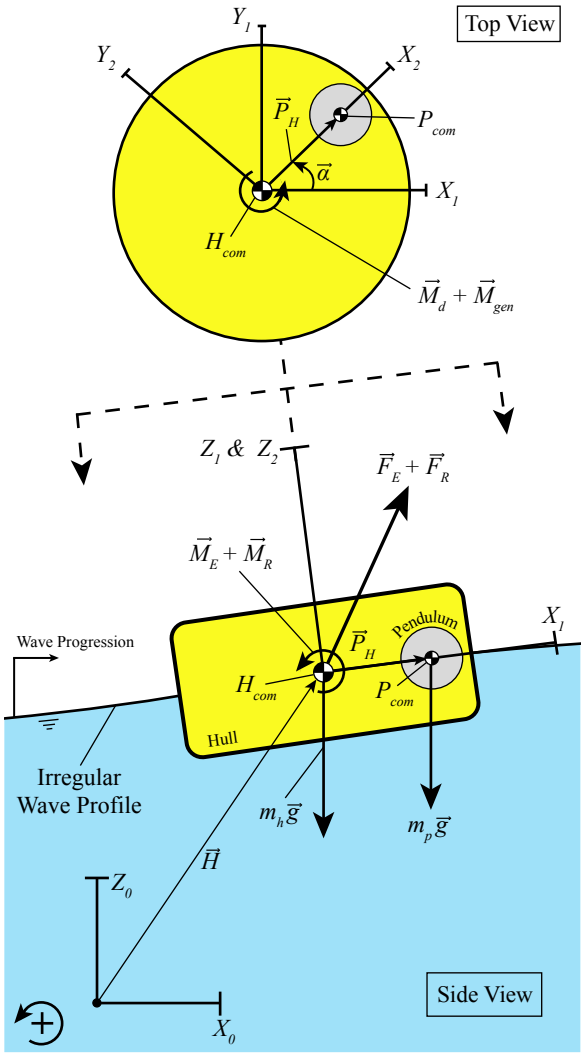

FIGURE 2. VAPWEC FREE BODY DIAGRAM

is given by

$$\ddot{H}_{z0} = \frac{-m_h\, g - m_p\, g + F_{E_{z0}} + F_{R_{z0}}}{m_h} \,. \tag{1}$$

The equation of motion for the hull rotating about the X_1 axis and the Y_1 axis, respectively, are given by

$$\dot{\omega}_{x_1} = \frac{M_{E_{x1}} + M_{R_{x1}} + R_{p_{y0}}\, m_p\, g}{I_{x1}} \tag{2}$$

and

$$\dot{\omega}_{y_1} = \frac{M_{E_{y1}} + M_{R_{y1}} - R_{p_{x0}}\, m_p\, g}{I_{y1}} \,. \tag{3}$$

The equations of motion defining the hull's orientation with respect to the global coordinate system (the hull's Euler angles) are given by

$$\dot{\phi} = \frac{\omega_{y_1}\cos(\psi) + \omega_{x_1}\sin(\psi)}{\sin(\theta)} \,, \tag{4}$$

$$\dot{\theta} = \omega_{x_1}\cos(\psi) - \omega_{y_1}\sin(\psi) \,, \tag{5}$$

and

$$\dot{\psi} = \frac{-\cos(\theta)\Big(\omega_{y_1}\cos(\psi) + \omega_{x_1}\sin(\psi)\Big)}{\sin(\theta)} \,. \tag{6}$$

The equation of motion defining the pendulum's rotation about the Z_1 axis is given by

$$\ddot{\alpha} = \frac{\sin(2\,\alpha)\left(\omega_{x_1}^2 - \omega_{y_1}^2\right)}{2} - \cos(2\,\alpha)\,\omega_{x_1}\,\omega_{y_1} + \frac{\Big(M_d + M_{gen} - L\,m_p\cos(\alpha+\psi)\sin(\theta)\,\left(g + \ddot{H}_{z0}\right)\Big)}{L^2\,m_p} \tag{7}$$

where

$$M_d = -C_p\,\dot{\alpha} \,, \tag{8}$$

and

$$M_{gen} = u(t) \,. \tag{9}$$

Note, control is to be implemented through generator feedback, see Eqn. (9). When M_{gen} opposes pendulum motion, electricity is being generated and energy is removed from the pendulum (generator mode). When M_{gen} aids the motion of the pendulum, energy is being transferred to the pendulum (motor mode).

Simulated Hydrodynamic Environment

The Pacific Northwest is a site of interest for WEC development, and as such the simulated irregular hydrodynamic wave environment is based on characteristics suitable for WEC development for Oregon State oceans. The irregular wave's spectrum is derived using the Modified Bretschneider-Mitsuyasu wave spectrum given by [12, 13]

$$S(f_j) = 0.205\; H_s^2\; T_s^{-4}\; f_j^{-5}\; \exp\left(-0.75\;\left(T_s\; f_j\right)^{-4}\right) \,. \tag{10}$$

The spectrum is generated using a significant wave height, H_s, of three meters and a significant wave period, T_s, of ten seconds. Such wave parameters can be considered the most appropriate and representative for WEC development off the coast of Oregon [9]. The resulting irregular wave form developed from the spectrum is due to the superposition of individual, monochromatic water surface elevations, η_j, and is given by

$$\vec{\eta}_{irr} = \sum_{j=1}^{N} \vec{\eta}_j = \sum_{j=1}^{N} \cos(k_j x_0 - 2\pi f_j t - \delta_j) \; . \tag{11}$$

For the generic VAPWEC simulations, a simple method is used for determining both the excitation force, $\vec{F}_E$, and the excitation moment, $\vec{M}_E$. The method leverages Froude–Krylov forcing and, is thus directly related to Eqn. 11. This method assumes a floating body to have negligible diffraction effects. Such an assumption is valid if the floating body is relatively small when compared to the wave's dominant wavelength and also valid when only a first order approximation of the excitation force is needed—as is the case for this work [14–17]. To facilitate the Froude–Krylov criterion, the modeled VAPWEC hull has a height of 2.5 meters and a diameter of 10 meters. The established hull size is much smaller than the irregular wave's 150 meter approximate significant wavelength, and is also large enough that viscous effects (due to flow separation) can be neglected [16, 17]. Ultimately, the needed excitation force, $\vec{F}_E$, and moment, $\vec{M}_E$, can be obtained through use of the aforementioned Froude–Krylov method by integrating the irregular wave's pressure field over the wetted surface area of the VAPWEC,

$$p_{irr} = \sum_{j=1}^{N} -\rho\, g\, z_0 + \rho\, g \eta_j K_{p_j} \tag{12}$$

where

$$K_{p_j} = \frac{\cosh\left(k_j(h+z_0)\right)}{\cosh(k_j h)}. \tag{13}$$

To simplify the integration of the pressure field over the continually changing wetted surface area of the modeled VAPWEC, the process is approximated by dividing the hull into four (A, B, C, and D) symmetric wedges, with each wedge having its own excitation force, see Figure 3. The respective excitation force of each wedge is a product of two components: (i) one fourth the weight of the hull and (ii) a scaled sigmoid function. The combination of these two components result in the following equation:

$$\vec{F}_N = \left(\frac{m_h\, g}{4}\right) \left(\frac{2}{1+\exp(-A_f\, \vec{d}_N)}\right)$$

$$= \frac{m_h\, g}{2\left(1+\exp(-\vec{d}_N)\right)} \tag{14}$$

where

$$N = A, B, C, D \; ,$$

$$\vec{d}_N = \vec{\eta}_N - \vec{R}_{N_{z0}} \; , \tag{15}$$

and

$$\vec{\eta}_N = \vec{\eta}_{irr}\left(x0 = R_{N_{x0}}\right) \; . \tag{16}$$

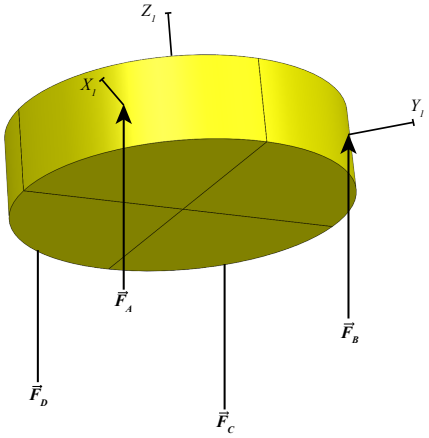

FIGURE 3. VAPWEC HULL WEDGES AND CORRESPONDING WAVE EXCITATION FORCES

The value of the sigmoid scaling function is what ultimately approximates the pressure field integration process and whose value is determined by how much a respective wedge is submerged below the irregular wave profile, $\vec{\eta}_{irr}$, see Figure 4. The sigmoid scaling function acts such that when the hull is half way submerged in still water, the sum of each wedge's excitation force is equal to the total weight of the VAPWEC's hull. Thus, the hull's nominal hydrostatic condition, without the pendulum, is half submergence. As each wedge's submergence inevitably increases or decreases, due to the hull being subjected to the irregular wave, $\vec{\eta}_{irr}$, and the pendulum dynamics, $\vec{\alpha}$, the contribution of each respective wedge excitation force is adjusted accordingly. In other words, as a wedge becomes increasingly more submerged, its corresponding excitation force is increased, but only until the wedge is completely submerged. After complete submergence, the wedge's corresponding excitation force no longer increases. Likewise, when a wedge becomes decreasingly less submerged, its corresponding excitation force is decreased, and can be decreased until zero which represents the

point where the majority of the wedge is unsubmerged. See Figures 3 and 4. Based on comparable ANSYS AQWA® analyses, this sigmoid function approximation technique gives the approximate excitation force, $\vec{F}_E$, and moment, $\vec{M}_E$ sufficient for this work:

$$\vec{F}_E = \vec{F}_A + \vec{F}_B + \vec{F}_C + \vec{F}_D \,, \tag{17}$$

and

$$\vec{M}_E = \sum_{N=A}^{D} \left(\vec{R}_N \times \vec{F}_N \right) . \tag{18}$$

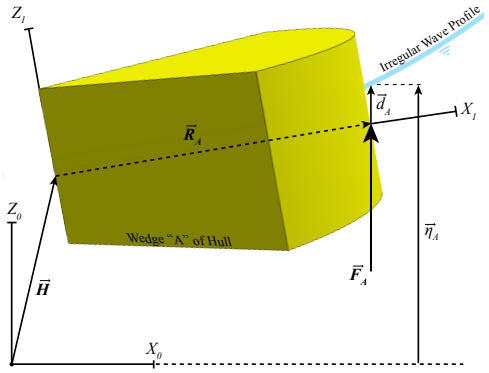

FIGURE 4. WEDGE "A" OF VAPWEC HULL

The radiation force, $\vec{F}_R$, and moment, $\vec{M}_R$, were found using a method from [18] and further supplemented by ANSYS AQWA®. ANSYS AQWA® was not solely used for the analysis in this work due to its several inabilities to handle advanced control algorithms such as what will be describe in a subsequent section. Note, the radiation force and moment can be expanded and related to the constrained motion of the modeled VAPWEC by the following:

$$\vec{F}_{R_{z_0}} = -C_{z0}\,\vec{\dot{H}}_{z0} - A_{z0}\,\vec{\ddot{H}}_{z0} \,, \tag{19}$$

$$\vec{M}_{R_{x1}} = -C_{x1}\,\omega_{x1} - Ax1\,\dot{\omega}_{x_1} \,, \tag{20}$$

$$\vec{M}_{R_{y1}} = -C_{y1}\,\omega_{y_1} - A_{y1}\,\dot{\omega}_{y1} \,. \tag{21}$$

A summary of the hydrodynamic and VAPWEC parameters used in this work are given in Table 1.

Active Controller Design

Using both model predictive and integral error control, a controller is developed to enforce a strategy that optimizes wave energy to electricity conversion. Such a controller is ideally suited for this problem due to its ability to cope with approximated nonlinear dynamics, its capacity to track desired pendulum state trajectories, and its allowance for wave profile prediction [5, 6, 19].

TABLE 1. SUMMARY OF HYDRODYNAMIC AND VAPWEC PARAMETERS

Parameter	Value
Significant Wave Height	3 [m]
Significant Wave Period	10 [s]
Hull Mass	10000 [kg]
Hull Principal moment of inertia about X_1	129709 [kg m^2]
Hull Principal moment of inertia about Y_1	129709 [kg m^2]
Hull Diameter	10 [m]
Hull Height	2.5 [m]
Sigmoid Approximation Factor	1
Pendulum Arm Length	3 [m]
Pendulum Mass	250 [kg]
Pendulum Damping Coefficient	0.1 [kg m^2 s^{-1}]
Hull Added Mass in Heave	109346 [kg]
Hull Added Inertia in Roll	385027 [kg m^2]
Hull Added Inertia in Pitch	385027 [kg m^2]
Radiation Damping in Heave	51252 [kg s^{-1}]
Radiation Damping in Roll	2578 [kg m^2 s^{-1}]
Radiation Damping in Pitch	2578 [kg m^2 s^{-1}]

The model predictive control aspect grants the controller a means to continually update the approximation of the nonlinear pendulum dynamics in a manner that allows for the application of linear optimal control theories for discrete moments in time. Such approximation enables the direct use of common linear control methods which are easily computed and implemented. Moreover, model predictive control provides a means for future research in which temporal and spacial wave profile prediction can occur [7]. With integral error control, the controller has the ability to track a desired ideal pendulum state trajectory. The controller combines the model predictive and integral error control aspects via an augmented state-space equation and a corresponding cost function that is analogous to linear quadratic regulator (LQR) problems.

A linear approximation to the pendulum dynamics in (7) can be written in a time-varying form that uses the current time window's (t_i) state values:

$$\dot{\boldsymbol{\Upsilon}}(t) = \boldsymbol{A}_{mpc}(t)\,\boldsymbol{\Upsilon}(t) + \boldsymbol{B}\,u(t) \tag{22}$$

where

$$\boldsymbol{A}_{mpc}(t) = \begin{bmatrix} \frac{-C_{x1}}{I_{x1}} & 0 & 0 & 0 \\ 0 & \frac{-C_{y1}}{I_{y1}} & 0 & 0 \\ 0 & 0 & 0 & 1 \\ A_{41}(t_i) & A_{42}(t_i) & A_{43}(t_i) & \frac{-C_p}{L^2 m_p} \end{bmatrix}, \quad (23)$$

$$A_{41} = \frac{\sin\left(2\,\alpha(t_i)\right)\omega_{x_1}(t_i)}{2}\,, \quad (24)$$

$$A_{42} = \frac{\cos\left(2\,\alpha(t_i)\right)\omega_{x_1}(t_i) - \sin\left(2\,\alpha(t_i)\right)\omega_{y_1}(t_i)}{2}\,, \quad (25)$$

$$A_{43} = \frac{\sin(\alpha(t_i)+\psi(t_i))\,\sin\left(\theta(t_i)\right)\left(g + \frac{F_{Hz0}(t_i)}{m_h}\right)}{L}\,, \quad (26)$$

$$\boldsymbol{\Upsilon}(t) = \begin{bmatrix} \omega_{x_1}(t) & \omega_{y_1}(t) & \alpha(t) & \dot{\alpha}(t) \end{bmatrix}^T\,, \quad (27)$$

$$\boldsymbol{B} = \begin{bmatrix} 0 & 0 & 0 & \frac{1}{L^2 m_p} \end{bmatrix}^T\,, \quad (28)$$

and recalling $u(t) = M_{gen}(t)$.

The pendulum state matrix, $\boldsymbol{A}_{mpc}$, could include any information for the intention of prediction and approximation. Information such as: historic, current, predicted state information; historic, current, predicted control information; or predicted wave environment and hull forcing information. The inclusion and investigation of using of such information for $\boldsymbol{A}_{mpc}$, is a natural path for future research. As it stands, the linear approximation of $\boldsymbol{A}_{mpc}$ used in this work, only includes hull and pendulum state information from the current time window, t_i.

As noted earlier, pendulum control is effectuated through generator torque feedback. When the moment due to the generator, M_{gen}, opposes the pendulum's angular velocity, $\dot{\alpha}$, electricity is being generated. When the moment due to the generator, M_{gen}, aids the pendulum's angular velocity, $\dot{\alpha}$, the generator is acting as a motor and electricity is being consumed.

The control strategy enforced by the active controller is based on tracking a desired pendulum state trajectory, $r(t)$. The reference function $r(t)$ is found through an iterative process such that a favorable trajectory is found for the aforementioned simulated irregular ocean wave environment. A specific method for ascertaining $r(t)$ is described by Boren and its purpose is to inform the controller of proper pendulum orientation throughout time such that pendulum motion optimizes wave energy to electricity generation [5].

Tracking the ideal pendulum state trajectory, $r(t)$, is the primary role of the integral error component of the controller [5,20]. Such tracking involves the minimization of the pendulum's error dynamics given by

$$\dot{e}(t) = r(t) - \alpha(t). \quad (29)$$

When written in state–space form the error dynamics in Eqn. (29) becomes

$$\dot{e}(t) = -\boldsymbol{C}\,\boldsymbol{\Upsilon}(t) + r(t), \quad (30)$$

$$\boldsymbol{C} = \begin{bmatrix} 0 & 0 & 1 & 0 \end{bmatrix}. \quad (31)$$

Thus, the augmented state–space form for the controller is the combination of the approximated pendulum state-space dynamics and the integral error dynamics. The resulting augmented state-space form is given by

$$\begin{bmatrix} \dot{\boldsymbol{\Upsilon}}(t) \\ \dot{e}(t) \end{bmatrix} = \begin{bmatrix} \boldsymbol{A}_{mpc}(t) & \boldsymbol{0} \\ -\boldsymbol{C} & 0 \end{bmatrix} \begin{bmatrix} \boldsymbol{\Upsilon}(t) \\ e(t) \end{bmatrix} + \begin{bmatrix} \boldsymbol{B} \\ 0 \end{bmatrix} u(t) + \begin{bmatrix} \boldsymbol{0} \\ 1 \end{bmatrix} r(t) \quad (32)$$

or

$$\dot{\boldsymbol{\Upsilon}}_{aug}(t) = \boldsymbol{A}_{aug}(t)\,\boldsymbol{\Upsilon}_{aug}(t) + \boldsymbol{B}_{aug}u(t) + \begin{bmatrix} \boldsymbol{0} \\ 1 \end{bmatrix} r(t) \quad (33)$$

as in [20]. Note that the zero entries in the matrices above are sized appropriately; that is, they may represent vectors or sub–matrices with zero entries.

The controller is derived using a linear quadratic cost function given as

$$J_i = \int_{t_i}^{\infty} \boldsymbol{\Upsilon}_{aug}^T(t)\boldsymbol{Q}\boldsymbol{\Upsilon}_{aug}(t) + u^T(t)\,R\,u(t)\,\mathrm{d}t \quad (34)$$

with

$$\boldsymbol{Q} = \begin{bmatrix} \mathbf{0} & \mathbf{0} \\ \mathbf{0} & q \end{bmatrix} . \tag{35}$$

The terms R and q represent control weighting and error weighting respectively. Small R values allow for greater pendulum control to be implemented, and correspondingly, larger q values enforce closer tracking of the function $r(t)$. These weightings are typically "tuned" to achieve desired performance.

To ensure suitable control of the pendulum and sufficient tracking of $r(t)$, Eqn. (34) is minimized by solving its corresponding steady state algebraic Riccati equation

$$\mathbf{0} = -\boldsymbol{P}\boldsymbol{A}_{aug} - \boldsymbol{A}_{aug}^{T}\boldsymbol{P} - \boldsymbol{Q} + \boldsymbol{P}\boldsymbol{B}_{aug}R^{-1}\boldsymbol{B}_{aug}{}^{T}\boldsymbol{P} \tag{36}$$

at sequential time moments in time, t. Thus, $\boldsymbol{P}$ in fact depends on t. At each time t, its associated gain matrix, $\boldsymbol{K}(t)$, is derived by

$$-\boldsymbol{K}(t) = -R^{-1}\,\boldsymbol{B}_{aug}{}^{T}\,\boldsymbol{P}(t) , \tag{37}$$

and thus over the entire operating time,

$$u(t) = M_{gen}(t) = -\boldsymbol{K}(t)\boldsymbol{\Upsilon}_{aug}(t) . \tag{38}$$

SIMULATION RESULTS

Utilizing the same simulated irregular ocean wave, hydrodynamic environment, and VAPWEC parameters (see Table 1, Eqns. (1)–(9) and Eqns. (11)–(21)), the results of two simulations are now given. The first simulation places the modeled VAPWEC in the simulated ocean environment without active control enabled. The second simulation places the same modeled VAPWEC in the same simulated ocean environment, but with the active controller developed by Eqns. (22)–(38), enabled. The resulting net power produced from each simulation is compared and, in this fashion, the benefits of using active control are assessed. The governing evaluation of the active controller is based upon its ability to increase *net* power output as compared to its uncontrolled counterpart.

The duration of each simulation is 1200 seconds with only the last 100 seconds of power generation being considered for evaluation. In this way, the evaluation is based upon the fully developed interactions between the irregular wave environment and the VAPWEC's dynamics—disregarding the transient effects that occur during the sudden placement of a VAPWEC into an already existing dynamic ocean wave environment. Note, positive power represents electricity generation by the VAPWEC (generator mode), while negative power represents electricity consumption by the VAPWEC (motor mode).

Generic VAPWEC without Active Control

Without active control, a VAPWEC generates electricity at a linear rate. This rate is a product of a predetermined extraction coefficient, C_{gen}, and the VAPWEC pendulum's angular velocity, $\dot{\alpha}$. This relationship is given by

$$\vec{M}_{gen}(t) = C_{gen}\dot{\alpha}(t) . \tag{39}$$

Thus, for electricity generation to occur, C_{gen}, must be a negative value and also a quantity that facilitates the largest amount of electricity generation. The determination of C_{gen} is ordinarily based on the converter's physical parameters in addition to the dominant characteristics of the converter's ocean wave energy environment. In the case of this simulation, C_{gen} was found by iteratively subjecting the modeled VAPWEC to the same irregular ocean wave while searching through a range of C_{gen} values between -80000 and 0 $\left[\text{kg m}^2\ \text{s}^{-1}\right]$. From this process a value of -29091 $\left[\text{kg m}^2\ \text{s}^{-1}\right]$ was found to generate the largest amount of electricity for the uncontrolled VAPWEC during the last 100 seconds of simulation time.

The simulation results for the uncontrolled VAPWEC, for the last 100 seconds are summarized in Figure 5 and its corresponding power generation results are given in Table 2. As shown in the power plot of Figure 5, by having a negative extraction coefficient, C_{gen}, the VAPWEC without active control will always generate electricity during any pendulum motion. Moreover, greater electric power generation is associated with faster pendulum rotation, which is indicated by steeper slopes in the pendulum position plot of Figure 5 and implied by Eqn. (39). Mean net continuous power output for the last 100 seconds of simulation time was only 382 watts—small considering the large 10 meter diameter of the VAPWEC's hull. This small result, however, is due to the generic form of the modeled VAPWEC. If one were to optimize the VAPWEC hull's geometry and pendulum parameters, than greater power output, even for an uncontrolled VAPWEC, could be had. In any case, it is the purpose of this work to focus on the comparison between an uncontrolled and active controlled VAPWEC without favor towards a particular VAPWEC design or configuration.

TABLE 2. RESULTS: WITHOUT ACTIVE CONTROL

Parameter	Value
Generator Extraction Coefficient	-29091 $\left[\text{kg m}^2\ \text{s}^{-1}\right]$
Mean Net, Continuous Power (during last 100 seconds)	382 [W]
Max Net, Peak Power (during last 100 seconds)	1,757 [W]

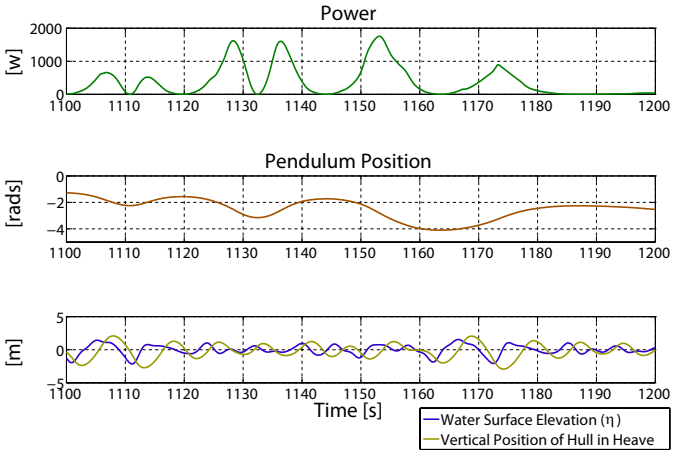

FIGURE 5. VAPWEC WITHOUT ACTIVE CONTROL

Generic VAPWEC With Active Control

To simulate an actively controlled VAPWEC, an optimal pendulum state trajectory, $r(t)$, must be identified. While there could be several possibilities for $r(t)$, for this simulation, a simple sinusoid was found to be an effective optimal pendulum state trajectory. The sinusoid is given by

$$r(t) = 3\sin(t)\ . \tag{40}$$

In addition to the optimal pendulum state trajectory, the active controller was forced to favor electricity generation over electricity consumption. Thus, whenever the controller sought to add energy to the system, it was only allowed to do so at 80 percent of its desired amount. The active control moment, $u(t)$, therefore, is given by

$$\begin{aligned} u(t) &= M_{gen}(t) \\ &= -\boldsymbol{K}(t)\boldsymbol{\Upsilon}_{aug}(t) \quad \text{when} \quad \pm M_{gen}\ \&\ \mp\dot{\alpha} \end{aligned} \tag{41}$$

and

$$\begin{aligned} u(t) &= 0.8\, M_{gen}(t) \\ &= -0.8\, \boldsymbol{K}(t)\boldsymbol{\Upsilon}_{aug}(t) \quad \text{when} \quad \pm M_{gen}\ \&\ \pm\dot{\alpha} \end{aligned} \tag{42}$$

When compared to the power results of the uncontrolled VAPWEC simulation (Figure 5 and Table 2), the results from the actively controlled VAPWEC simulation (see Figure 6 and Table 3) indicate both greater peak power outputs and continuous–mean power output. Due to the nature of active control however, electric power generation does not always occur. Thus, while active control produced large spikes—nearly 0.5 [MW]—of power at certain times, its continuous–mean power output was approximately 1.5 [kW]. Nonetheless, in terms of continuous–mean power output, the actively controlled VAPWEC outperforms its uncontrolled counterpart by nearly 1 [kW] of continuous–mean power output.

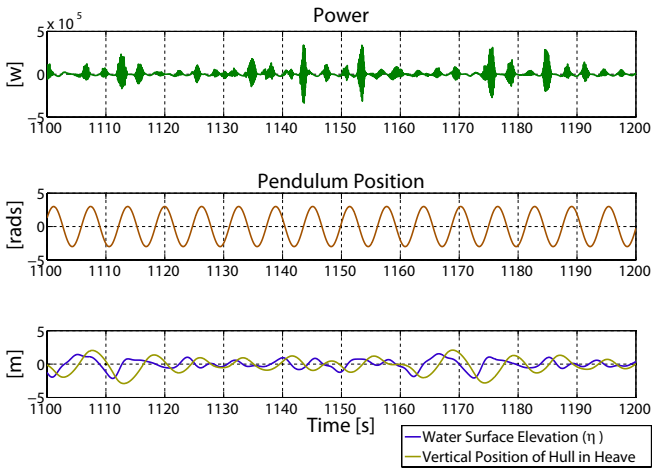

FIGURE 6. VAPWEC WITH ACTIVE CONTROL

TABLE 3. RESULTS: WITH ACTIVE CONTROL

Parameter	Value
Selected Optimal Pendulum State Trajectory	$r(t) = 3\sin(t)$ [m]
Error weighting q	1e13
Control weighting R	1e-11
Mean Net, Continuous Power (during last 100 seconds)	1,473 [W]
Max Net, Peak Power (during last 100 seconds)	493,080 [W]

CONCLUSIONS

In this paper, we have shown that net mean power generation for a VAPWEC could be increased by over 200% by utilizing an active controller based on model predictive and integral error tracking control theories. Such an approach to control design has been used by others for other technologies, and is a realistic first take for controlling both VAPWECs and wave energy converters in general [1, 5, 6].

Another contribution in this paper, is the simplified approach to modeling the hydrodynamic forcing on the device. Initially, panel methods and ANSYS AQWA® were used to both compute the hydrodynamic forces and apply active control to the VAPWEC [5, 21], but that approach proved to be entirely unwieldy due to AQWA's inadequate interface for active control techniques. The approach used in this paper is essentially a way to average the hydrodynamic forces over quadrants of the

VAPWEC, and could be refined by partitioning the device into more wedges.

A possible limitation regarding the use of such active control, are the resulting large power spikes. Here we assume an ideal power take–off system, a system capable of handling the transmission of power of up to nearly 500 kilowatts. However, these large power spikes need not be prohibitive, especially if such spikes are only allowed in generator mode (no need to source large amounts of power) and if they last for very brief time periods.

Another possible limitation regarding the use of active control, is the assumed forward knowledge of the incident, incoming irregular wave form. Such a limitation, however, could be surmounted through the use of state estimators that transmit wave telemetry to the controller such that the controller can make reasonable predictions about the future incident wave. Such estimators are currently being investigated by the authors of this work.

An additional area for future work in VAPWEC control design, involves utilizing cost functions that do not require tracking of an desired pendulum position, $r(t)$, but instead the controller would continually develop, in essence, $r(t)$, on–the–fly. Such real–time tracking function development is being investigated by the authors of this work.

ACKNOWLEDGMENT

The material in this paper is based upon work supported by the US Department of Energy under Award Number DEFG36-08GO18179.

REFERENCES

[1] Previsic, M., 2013. "The potential of wave power in the United States in an economic context". In Track 10: EWTEC 2014, The European Wave and Tidal Energy Conference.

[2] Bull, D., Ochs, M., Laird, D., Boren, B., and Jepsen, R., 2013. Technological cost-reduction pathways for point absorber wave energy converters in the marine hydrokinetic environment. Tech. rep., Sandia National Laboratories.

[3] Hinck III, E. C., 1966. Wave power generator, January. United States Patent: 3231749.

[4] Bretl, J. G., 2009. "A time domain model for wave induced motions coupled to energy extraction". PhD thesis, The University of Michigan.

[5] Boren, B. C., 2013. "On the modeling and control of horizontal pendulum wave energy converters". Master's thesis, Oregon State University, June.

[6] Brekken, T. K. A., 2011. "On model predictive control for a point absorber wave energy converter". *In PowerTech,* ***1***, pp. 1–8.

[7] Wang, L., 2009. *Model Predictive Control System Design and Implementation Using MATLAB®*. Advances in Industrial Control. Springer.

[8] Findeisen, R., Allgöwer, F., and Biegler, L., 2007. *Assessment and Future Directions of Nonlinear Model Predictive Control*. Lecture notes in control and information sciences. Springer.

[9] Lenee-Bluhm, P., 2010. "The wave energy resource of the U.S. pacific northwest". Master's thesis, Oregon State University.

[10] Altmann, S., 2005. *Rotations, Quaternions, and Double Groups*. Dover books on mathematics. Dover Publications.

[11] Kuipers, J., 1999. *Quaternions and Rotation Sequences: A Primer With Applications to Orbits, Aerospace and Virtual Reality*. Mathematical Sciences Series. Princeton University Press.

[12] Goda, Y., 2010. *Random Seas and Design of Maritime Structures (3rd Edition)*. Advanced series on ocean engineering. World Scientific Publishing Company, Incorporated.

[13] Goda, Y., 1988. "Statistical variability of sea state parameters as a function of a wave spectrum". *Coastal Engineering in Japan,* ***31***, pp. 39–52.

[14] Dean, R., and Dalrymple, R., 1991. *Water Wave Mechanics for Engineers and Scientists*. Advanced series on ocean engineering. World Scientific.

[15] Newman, J., 1977. *Marine Hydrodynamics*. Wei Cheng Cultural Enterprise Company.

[16] Sarpkaya, T., 2010. *Wave Forces on Offshore Structures*. Wave Forces on Offshore Structures. Cambridge University Press.

[17] Wilson, J., 2003. *Dynamics of Offshore Structures*. Wiley.

[18] Ghadimi, P., Bandari, H., and Rostami, A., 2012. "Determination of the heave and pitch motions of a floating cylinder by analytical solution of its diffraction problem and examination of the effects of geometric parameters on its dynamics in regular waves". *International Journal of Applied Mathematical Research,* ***4***, pp. 611–633.

[19] Rawlings, J., and Mayne, D., 2009. *Model Predictive Control: Theory and Design*. Nob Hill Publishing.

[20] Burl, J., 1999. *Linear optimal control: H_2 and H_∞ methods*. Addison Wesley Publishing Company Incorporated.

[21] Chakrabarti, S., 2005. *Numerical Models in Fluid-Structure Interaction*. Advances in Fluid Mechanics. WIT Press.